

ORIGINAL ARTICLE

DOI: <https://doi.org/10.30932/1992-3252-2023-21-4-5>World of Transport and Transportation, 2023,
Vol. 21, Iss. 4 (107), pp. 186–198

Methodology for Assessing Shortened ILS LOC and GP Critical Areas: an Example of Gorno-Altai Aerodrome



Evgeny A. RUBTSOV



Sergey A. KUDRYAKOV



Iakov M. DALINGER

Evgeny A. Rubtsov¹, Sergey A. Kudryakov², Iakov M. Dalinger³^{1, 2, 3}*Russian University of Transport, Moscow, Russia.*□ ¹ *rubtsov.rut.miit@yandex.ru.*□ ² *psi_center@mail.ru.*□ ³ *iakovdalinger@gmail.com.*¹ *SPIN-kod: 5832-3060, ORCID 0000-0003-2126-0015.*² *Scopus Author ID: 57194207063, ORCID 0000-0002-1303-3528.*³ *SPIN-kod: 8895-3700, Scopus Author ID: 57195278185, ORCID 0000-0002-7744-7156.*

ABSTRACT

Based on the analysis of recommendations of the International Civil Aviation Organization on a reasonable reduction in sizes of ILS critical areas and identification of shortcomings of the existing requirements of the Russian Federal Aviation Regulations for critical areas of ILS localiser and glide path (glide slope), a procedure has been developed that allows assessment localiser and glide slope bends for shortened critical areas. The assessment comprises the influence of different reflecting objects situated on operation area of the aerodrome, as well as of aerodrome environs on the operation of the ILS localiser and glide path.

Reflecting objects can be approximated by models of a wall (that simulates reflections from buildings, bridges, fences), of a cylinder (that simulates reflections from factory pipes, tanks, containers, aircraft fuselages) and of a hemispherical diffuse reflector (simulates reflection from elevated terrain).

The procedure was tested for Gorno-Altai aerodrome, and a proposal was developed to reduce the critical area of the localiser, which will expand the apron by 35 m, eliminate problems with imposed speed limits and blocking movement of aircraft on the taxiway. Also, the probability of service failure will decrease by 3...11 times, and the runway occupancy time will decrease by 12,5...26 % compared to existing features.

Keywords: air transport, flight safety, aerodrome, airfield, aircraft landing, ILS, critical area, aerodrome operation area.

For citation: Rubtsov, E. A., Kudryakov, S. A., Dalinger, I. M. Methodology for Assessing Shortened ILS LOC and GP Critical Areas: an Example of Gorno-Altai Aerodrome. World of Transport and Transportation, 2023, Vol. 21, Iss. 4 (107), pp. 186–198. DOI: <https://doi.org/10.30932/1992-3252-2023-21-4-5>.

*The text of the article originally written in Russian is published in the first part of the issue.
Текст статьи на русском языке публикуется в первой части данного выпуска.*

INTRODUCTION

Air transport remains one of the leading sectors of the Russian economy. The current stage of development of aviation technology is characterised by widespread introduction of modern radio and electronic instruments to ensure flight safety. Statistics show that about 60 % of aviation accidents occur during approach and landing of aircraft [1]. Therefore, especially high requirements address radio engineering landing systems, namely, the most widely used ILS (instrument landing system). ILS can provide precision landing for [facility performance] categories I, II and III A.¹

To form the required radiation pattern of the ILS antennas and minimise the multipath interference caused by reflection of radio waves from local objects, specially regulated and critical areas are introduced. According to the recommendations of the International Civil Aviation Organization (ICAO), it is also necessary to consider sensitive areas.²

Within the regulated areas, requirements are imposed on the microrelief and slope of the terrain, as well as on the height of vegetation or snow cover. The dimensions of those areas are provided for in the technical documentation developed by the manufacturer of the ILS system.

¹ Kudryakov, S. A., Kulchitsky, V. K., Povarenkin, N. V. [et al] Radio engineering support for aircraft flights and aviation telecommunications [Radiotekhnicheskoe obespechenie poletov vozdukhnykh sudov i aviatsionnaya elektrosvyaz]. Moscow, LLC Scientific Publishing Center INFRA-M, 2021, 299 p.

² Annex 10 to the Convention on International Aviation. Aeronautical telecommunications. Vol. 1. Radio navigation aids. Seventh edition, ICAO, July 2018, 658 p.

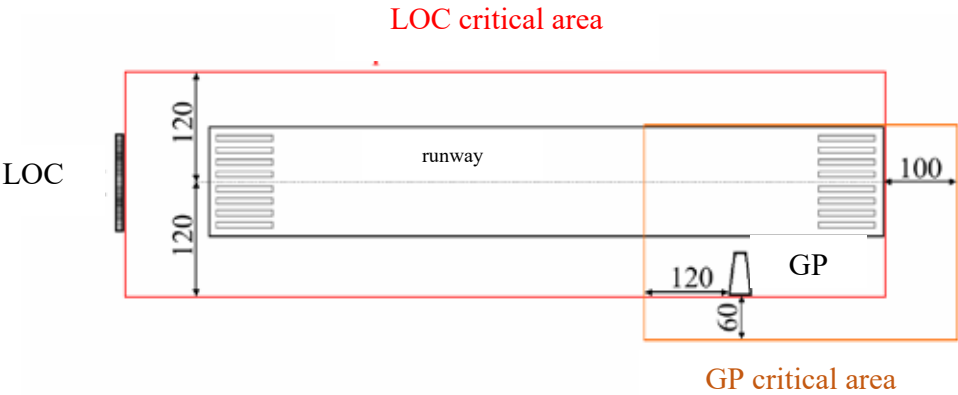
The presence of any objects (except for lighting equipment stands) within the critical area is prohibited, as this affects the safety of the landing approach. Objects located within the sensitive area may affect safety and are undesirable. At Russian aerodromes, sensitive areas are not taken into account. The dimensions of the ILS localizer and glide path critical areas are provided for in the federal aviation regulations «Radio technical support for aircraft flights and aviation telecommunications in civil aviation» (FAP-297) (Pic. 1).

The disadvantage of the existing requirements is that the dimensions of the critical areas are constant, and their change is possible only in case of moving the position of the LOC or GP, changes in the runway parameters (moving the threshold, changing the width), as well as when entering a new glide path angle.

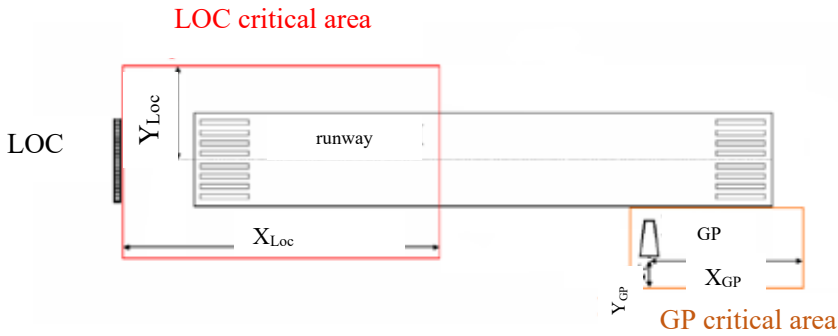
At the same time, ICAO recommends reducing dimensions of critical and sensitive areas of modern ILS systems and making their boundaries changeable depending on the size of the objects adverse to the area.

ICAO documents² contain figures of the LOC and GP critical areas (summarised in Pic. 2). The sizes of the zones (X_{Loc} , Y_{Loc} , X_{GP} , Y_{GP}) are not constant and depend on the type of interfering object (car, aircraft) and its dimensions, as well as on the type of ILS antenna system.

The ICAO recommendation to reduce the size of critical areas is reasoned by the need to increase the capacity of the aerodrome by reducing the time it takes aircraft to taxi onto the runway, increasing the number of parking stands, as well as by optimising traffic of cars and special vehicles along taxiways. In this case, it is



Pic. 1. LOC and GP critical areas (dimensions are given in meters) in accordance with the requirements of FAP-297.



Pic. 2. LOC and GP critical areas according to ICAO recommendations.

recommended to model the impact of objects on operation of the ILS system and conduct special flight checks to confirm the required level of flight safety.

Therefore, the task is to develop methods for determining the size of critical areas, allowing to minimise the flight check program, and in some cases, abandon them, is quite relevant.

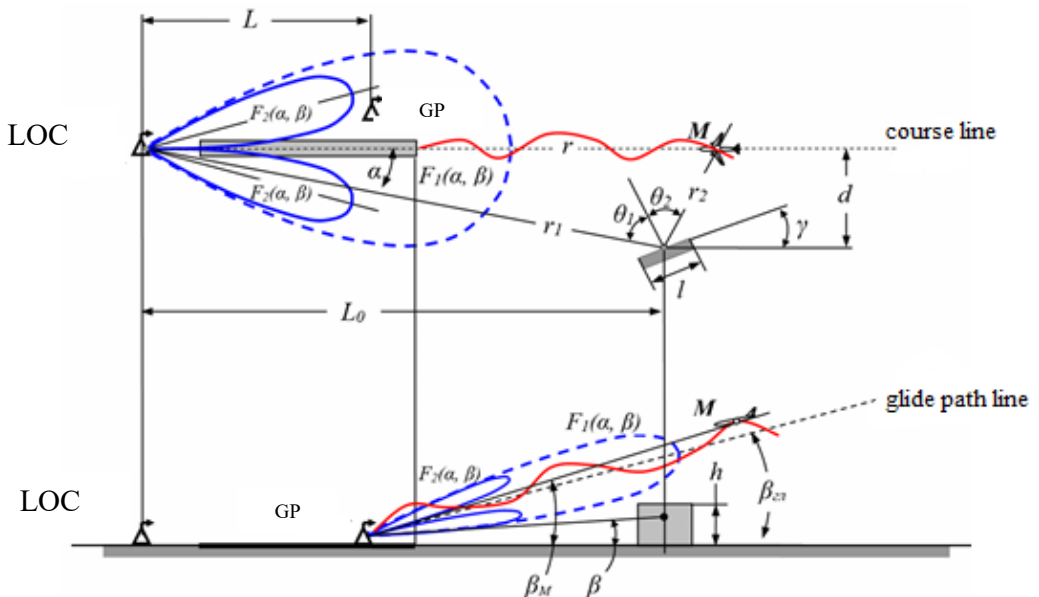
The objective of the research, described in the article, is development of a methodology for assessing the influence of objects located on the aerodrome movement area, which makes it possible to identify the size of the ILS critical area in accordance with ICAO recommendations.

METHODS AND MATERIALS

The LOC and GP operation can be influenced by signals reflected by various objects located in

the area near the aerodrome [2; 3], as well as on its operations area [4]. The reflecting object can influence the operation of the ILS LOC and GP, which is expressed in the observed curving of the indicated landing trajectory (course line and glide path). The magnitude of the curvature is determined by calculating the deviation from the values of the difference in the depth of modulation (DDM) at points of the indicated landing trajectory. A schematic representation of curved course line and glide path is shown in Pic. 3 [4].

The field strength of the direct and reflected signals at the reception point (point M in Pic. 3) is determined by the shape of the ILS antenna radiation pattern. For ILS antennas with assigned zero PCV values, this is a single main lobe plot $F_1(\alpha, \beta)$ (for the sum signal channel) and a double lobe plot $F_2(\alpha, \beta)$ (for the differential signal



Pic. 3. Curvature of the ILS course lines and glide path, caused by the multipath of the signals.

channel), where α is the angle in the horizontal plane measured from the runway axis; β – angle in the vertical plane, measured upward from the runway threshold.

The magnitude of DDM at the reception point M (Pic. 3) in the presence of some i -th reflecting object is determined by the expression [4–8]:

$$DDM = m \frac{E_{m2}}{E_{m1}} \cdot \frac{F_2(\alpha, \beta_M) + F_2(\alpha, \beta) k_{\text{ref}} \cos \psi_i}{F_1(\alpha, \beta_M) + F_1(\alpha, \beta) k_{\text{ref}} \cos \psi_i}, \quad (1)$$

where m – amplitude modulation ratio (0,2 for LOC and 0,4 for GP);

E_{m2} / E_{m1} – ratio of field strengths created by the differential and sum channels;

A – angle in the horizontal plane, measured from the runway axis, degrees;

β – elevation angle of the reflecting object observed from the location of ILS antennas, degrees;

β_M – elevation angle of point M observed from the location of the ILS antennas, degrees;

k_{ref} – reflection coefficient;

h – height of the phase centre of the radar antenna, m;

Ψ – phase shift between direct and reflected signals from the object at point M , degrees.

In case of flight along a glide path, the angle θ will be equal to zero, and the angle β will be equal to the angle of inclination of the glide path (β_0). Then the curvatures expressed in DDM are defined as [4–8]:

1) for LOC:

$$DDM = m \frac{E_{m2}}{E_{m1}} \cdot \frac{F_2(\alpha; \beta) \cdot \rho \cdot \frac{r}{r_1 \cdot r_2} \cdot \cos \psi}{F_1(0; \beta_0) + F_1(\alpha; \beta) \cdot \rho \cdot \frac{r}{r_1 \cdot r_2} \cdot \cos \psi}, \quad (2)$$

2) for GP:

$$DDM = m \frac{E_{m2}}{E_{m1}} \cdot \frac{F_2(\alpha; \beta) \cdot \rho \cdot \frac{r}{r_1 \cdot r_2} \cdot \cos \psi}{1 + F_1(\alpha; \beta) \cdot \rho \cdot \cos \psi}, \quad (3)$$

where ρ is reflection coefficient modulus.

RESULTS

1. The Proposed Methodology and Algorithm for its Application

The field strength of the reflected signal depends on the properties of the object, which are characterised by geometric dimensions and reflection coefficient. Different types of re-emitters are characterised by their reflection modulus ρ , so they form the reflected signal in different ways and affect the overall pattern of re-reflections. The amount of curvature is proportional to the reflection coefficient

$k_{\text{ref}} = \rho \times r / (r_1 + r_2)$, which will be greater with larger reflecting object's area and the value of $r / (r_1 + r_2)$.

In the simplest case, objects can be approximated by such models as a wall (simulates reflections from buildings, bridges, fences), a cylinder (simulates reflections from factory pipes, tanks, containers, aircraft fuselages) and a hemispherical diffuse reflector (simulates reflection from elevated terrain). As a rule, there are several different types of objects in the LOC and GP radiation area. The total distortion is the sum of distortions from a set of elementary reflecting objects [4].

To assess the reflective properties of objects, it is advisable to determine their effective scattering area (ESA). The value of ESA of a reflecting object is determined by the shape (size) of the object, the materials used (reflective, absorbing, radiotransparent ones), production technology (smoothness of the outer surface, the presence of steps, cutouts, slits). In general, ESA is defined as [9]:

$$\sigma = 4\pi \lim_{R \rightarrow \infty} R^2 \frac{E_s^2}{E_0^2}, \quad (4)$$

where E_0 – the magnitude of the electrical component incident from the source onto the object of the electromagnetic field;

E_s – the magnitude of the electrical component of the scattered electromagnetic field at the receiving point;

R – distance from object to emitting source.

The greatest contribution to ESA is made by the area and shape of the reflecting object. There are objects of simple shapes and complex shapes.

Let us consider methods for calculating ESA of reflectors of simple shapes (Table 1), which can be used, among other things, for preliminary assessment [9].

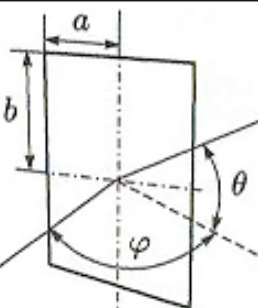
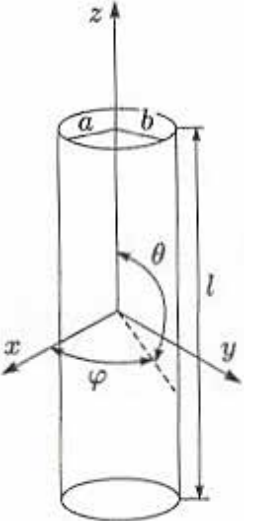
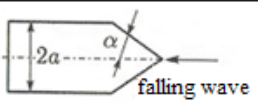
Currently, at airfields there may be objects made of radiotransparent materials (for example, hangars or fuselages of modern aircraft made of composite materials). Inside these objects there are various reflective elements (cables, equipment, metal structural elements – for aircraft; load-bearing structures in the form of metal trusses – for hangars). Therefore, it is relevant to calculate the scattering characteristics of such complex objects.

The internal metal structures of complex objects can be represented in the form of ideally conducting elements, as shown in Pic. 4 [10].



Table 1

Methods for assessing ESA of reflecting objects with simple shapes

Reflector	Geometry	Formula	Remark
Rectangular plate		$\sigma = \frac{64\pi a^2 b^2}{\lambda^2}$ $\sigma = \frac{114a^6}{\lambda^4}$	When $\lambda \ll a$, $\lambda \ll b$ For $\theta = 90^\circ$, $\varphi = 0^\circ$ When $a=b$, $\lambda \gg a$ For $\theta = 90^\circ$, $\varphi = 0^\circ$
Cylinder		ESA of a round cylinder: $\sigma = \frac{2\pi l^2 a}{\lambda}$ ESA of an elliptic cylinder: $\sigma = \frac{2\pi l^2 b^2}{\lambda a}$ ESA of an elliptic cylinder: $\sigma = \frac{2\pi l^2 a^2}{\lambda b}$	When $\lambda \ll l$, $\lambda \ll a$, $\lambda \ll b$ For $\theta = 90^\circ$, $\varphi = 0^\circ$ For $\theta = 90^\circ$, $\varphi = 90^\circ$
Cone cylinder		$\frac{\sigma}{\pi \cdot a^2} = \frac{4\pi}{(\pi + \alpha)^2} \times \sin^2\left(\frac{\pi^2}{\pi + \alpha}\right) \times \frac{1}{\left[\cos\left(\frac{\pi^2}{\pi + \alpha}\right) - \cos\left(\frac{2\pi^2}{\pi + \alpha}\right)\right]^2}$	For $\theta = \varphi = 0^\circ$ reflecting object's dimensions are larger than wavelength

It is also advisable to use a combined modelling method, taking into account the dielectric (radiotransparent) and ideally conducting elements of a complex object. Ideally conducting scattering elements can be divided into two groups [10–12]: smooth surfaces (approximated by sections of triaxial ellipsoids) and edge local scattering areas (approximated by break lines).

The break line of a surface (a section of a flat curve) is approximated by a section of an ellipse, and the edge of a straight break is approximated by a straight line's segment. The number of

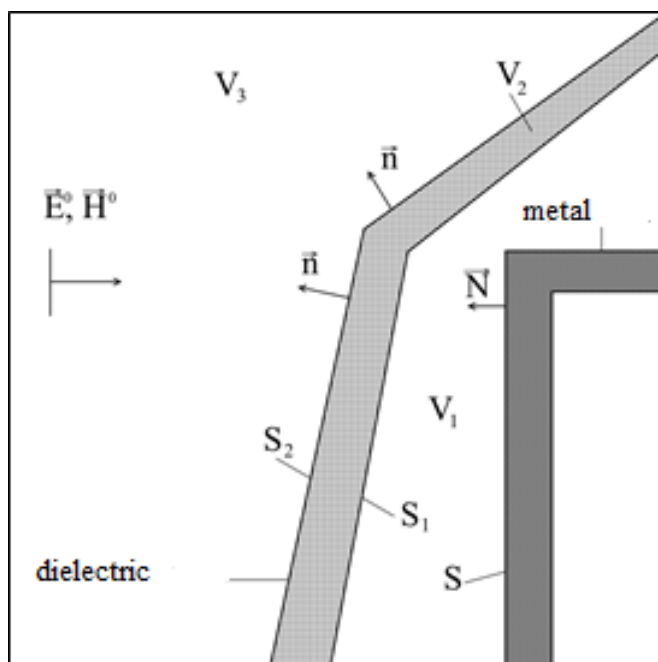
ellipsoids for each complex object is selected individually. Let a complex object be irradiated by a plane wave [10–12]:

$$\begin{aligned} \vec{E}^0(\vec{x}) &= \vec{p} e^{jk_0(\vec{R}^0 \cdot \vec{x})}; \\ \vec{H}^0(\vec{x}) &= \sqrt{\frac{\epsilon_0}{\mu_0}} \left(\vec{R}^0 \times \vec{p} \right) e^{jk_0(\vec{R}^0 \cdot \vec{x})}, \end{aligned} \quad (5)$$

where \vec{p}^0 – radio wave polarisation unit vector;

\vec{R}^0 – unit vector of the direction of radio wave propagation;

ϵ_0, μ_0 – absolute dielectric and magnetic permeabilities of free space;



Pic. 4. Model of a complex object (using the example of a hanger).

k_0 – wavenumber in free space ($k_0 = 2\pi / \lambda$,
 λ – incident monochromatic wavelength);
 \vec{x} – radius vector of the currently analysed point.

The field of an auxiliary point source (dipole) in the presence of only region V_2 (outer dielectric shell) is defined as $\vec{\xi}(\vec{x}|\vec{x}_0, \vec{p})$ and $\vec{H}(\vec{x}|\vec{x}_0, \vec{p})$, where \vec{x}_0 – the radiation source location point, \vec{p} – its moment vector.

To obtain the scattered field from the complex object under consideration, we apply the expression [10–12]:

$$\vec{p} \cdot \vec{E}^p(-\vec{R}^0) = \vec{p} \cdot \vec{\xi}(-\vec{R}^0) + \frac{1}{j\omega\epsilon_0} \int_S \vec{I}(\vec{x}) \cdot \vec{\xi}(\vec{x}|\vec{R}^0, \vec{p}) dS, \quad (9)$$

where $\vec{\xi}(-\vec{R}^0)$ – field scattered only by the outer dielectric shell in the absence of ideally conducting elements underneath it;

$\vec{\xi}(\vec{x}|\vec{R}^0, \vec{p})$ – tangential component of the plane wave field (with respect to the surface of ideally conducting elements S) propagating in the direction \vec{R}^0 and having passed through the dielectric shell, at point \vec{x} on the surface of ideally conducting elements S ;

$\vec{I}(\vec{x})$ – surface current density on S induced by a plane wave having passed through the dielectric shell (\vec{E}^0, \vec{H}^0);

\vec{p} – unit vector of polarisation direction of a plane wave.

The integral term in this expression gives the contribution of ideally conducting elements (under the dielectric shell) to the total scattering field, taking into account intra-system electrodynamic interactions. Considering that a complex object usually has large electrical dimensions, the terms on the right side can be calculated approximately using the short-wave diffraction method. The method for determining the field reflected from complex objects is described in more detail in [10–12].

After calculating the curvature of the course line and glide path, it is necessary to process the results. It is advisable to analyse the amplitude of the curvature of the glide path line from the border of the GP coverage area, at a distance of 18,5 km from the end of the runway, and the amplitude of the curvature of the course line – approximately from the border of the coverage area of the wide channel of the LOC, located at a distance of 32 km from it. Within the analysed area, it is necessary to determine the intervals at which the amplitude of the curvature exceeds the maximum permissible value and sum them up. If the total length of these sections exceeds 5 % of the length of the analysed interval, then the accuracy requirements for this channel are not met.

It is impossible to completely eliminate the influence of re-reflected signals on operation of





Pic. 5. Satellite image of the runway of Gorno-Altai aerodrome indicating the GP and LOC critical areas, as well as reflecting objects (a hill and buildings).

the ILS system, therefore ICAO has introduced restrictions on the permissible magnitude of curvature of indicated trajectories, depending on the distance to the runway threshold and the category of the ILS.³

Thus, the application of the proposed methodology can be described with the following algorithm:

1) Analysis of the environs of the aerodrome and assessment of the curvature of the course and glide path lines in the presence of buildings, structures and elevated terrain.

2) Comparison of simulation results with data from ILS flight checks to verify the adequacy and accuracy of the applied method in specific conditions.

3) Performing an assessment of the influence of objects located near the boundaries of critical areas (defined according to FAP-297), but not interfering it to confirm the given ILS category.

4) Performing an assessment of the influence of objects located within the boundaries of critical areas (defined according to FAP-297). The placement of objects can be along the boundaries of areas recommended by ICAO, or at the required boundaries, based on technological need.

5) Based on the modelling results, it is necessary to conclude whether it is possible to reduce the size of the ILS critical area in accordance with ICAO recommendations.

When performing steps 3 and 4, it is necessary to carry out modelling for various angles of rotation of objects relative to the ILS antennas. Subsequent assessment and development of solutions should be carried out for the worst case of the object's influence on the operation of

landing systems (the largest curvature of the course line or glide path). It is advisable to confirm the simulation results during flight checks.

2. Approbation of the Developed Algorithm

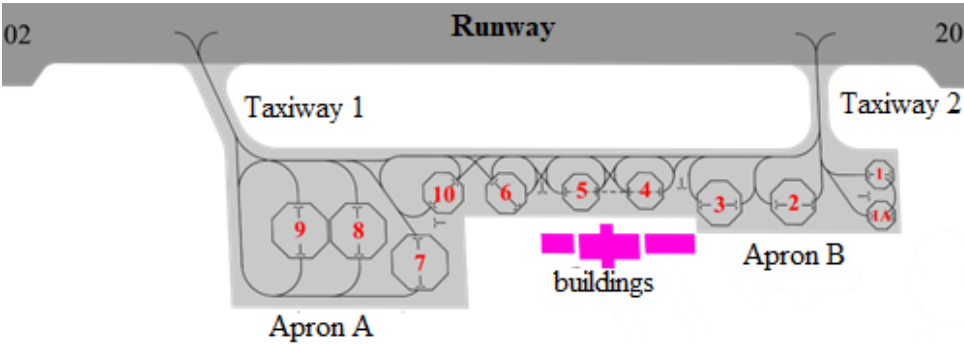
Let us apply the developed algorithm for assessment of the possibility of reducing the size of the ILS critical area at Gorno-Altai aerodrome, located in Altai Republic. The aerodrome has one runway with a length of 2031 m, equipped with single-directional ILS of category I, the glide path angle is $3^{\circ}20'$. Pic. 5 shows a satellite image of the runway, indicating the location of GP and LOC, reflecting objects and LOC and GP critical areas (according to FAP-297).

Analysis of the aerodrome area (Pic. 5) showed the presence of a hill in transit of the runway, and buildings near the runway itself, which could affect the operation of LOC. The LOC critical area affects movement of traffic along the taxiway and the placement of aircraft in parking areas.

The collection of Aeronautical Information Publications (AIP)⁴ notes that there are a number of restrictions and features regarding aircraft taxiing (Pic. 6). Thus, after landing of aircraft index 3–6 on Runway 20, a 180° turn may be performed only at reduced speed and at the threshold of Runway 02, using the widening. Taxiing along the apron along occupied parking stands 2 and 3 is permitted for aircraft with a wingspan of no more than 29 m. Taxiing along the apron along when PS4–PS6 and PS10 are occupied is permitted for aircraft with a wingspan of no more than 24 m. Also, the AIP provides for a number of restrictions on taxiing of aircraft

³ Methodological recommendations [of the Ministry of Transport of the Russian Federation] for flight inspections of ground-based radio technical support for flights, aviation telecommunications and airfield lighting systems. Appendix IL No. 79r., 2012

⁴ AIP collection of aeronautical information publications of the Russian Federation. Part III Aerodromes (AD). [Electronic resource]: <http://www.caiga.ru/common/AirInter/validaip/html/rus.htm>. Last accessed 26.05.2023.



Pic. 6. Map of aircraft parking areas at the Gorno-Altai aerodrome.

with a certain wingspan (more than 25–29 m) when PS2–PS6 and PS10 are occupied. These restrictions are due to the fact that the width of the apron cannot be increased without interfering the LOC critical area.

In the current configuration, when taxiing even medium (CRJ200) and small (L410) aircraft, from 3 to 5 parking stands out of total 11 available PSs should be free, which increases a probability P of refusing to serve the next aircraft on the apron⁵:

$$P = \frac{\left(\frac{I_e T_n}{2}\right)^{N_n} \frac{1}{N_n!}}{\sum_{m=0}^{N_n} \left(\frac{I_e T_n}{2}\right)^m \frac{1}{m!}}, \quad (7)$$

where I_e – aircraft traffic intensity at the estimated hour;

T_n – average time of aircraft parking on the apron;

N_n – number of parking stands on the apron;

m – number of simultaneously occupied parking stands.

The average time of aircraft parking on the apron can be found from table 2. For Gorno-Altai aerodrome, T_n is assumed to be 0,84 hours.

Equation (7) can be solved for each group of aircraft, and averagely for all groups. Considering that the overwhelming number of

takeoff and landing operations (TOL) at Gorno-Altai aerodrome are performed by aircraft of groups II–IV, we obtain a minimum probability of service failure in the range of 0,0112...0,0126 (at a TOL intensity of 10 aircraft/h) and 0,158...0,315 (at TOL intensity of 15 aircraft/h).

Taxiing speed restrictions affect runway occupancy times. Thus, when an aircraft takes off, the occupancy time $T_{takeoff}$ is estimated as:

$$T_{takeoff} = t_{taxi} + t_{th} + t_{run} + t_{ag} \quad (8)$$

where t_{taxi} – time of taxiing to the line-up position;

t_{th} – time of stay of the aircraft at the line-up position to bring the engine thrust to takeoff mode;

t_{run} – aircraft takeoff run time;

t_{ag} – time of acceleration and gaining the altitude.

When landing an aircraft, the occupancy time T_{land} is estimated as:

$$T_{land} = t_{gl} + t_{lrun} + t_{ltaxi} \quad (9)$$

where t_{gl} – aircraft gliding time from the decision altitude until touching down the runway;

t_{lrun} – aircraft landing run time;

t_{ltaxi} – time of aircraft taxiing after landing beyond the side boundary of the runway (outside the LOC critical area).

To carry out the assessment calculation, we will accept typical values of the indicated time intervals characteristic of Gorno-Altai aerodrome (Table 3). The values of taxiing to the line-up position and taxiing after landing are

Table 2

Duration of aircraft parking on the apron

Aircraft group	Duration of aircraft parking on the apron with regard to different types of flights			
	Transit	Return	Final destination	Origin departure
I	1,50	2,10	0,90	0,90
II	1,00	1,20	0,80	0,90
III–IV	0,55	0,75	0,40	0,80

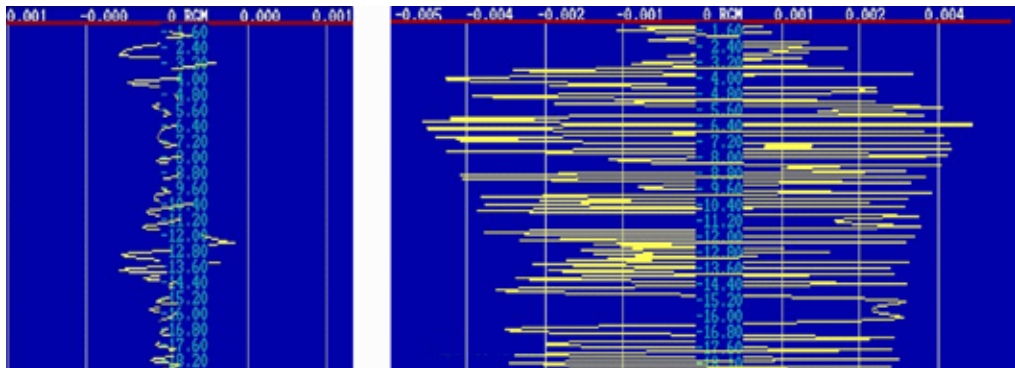
⁵ Glushkov, G. I., Babkov, V. F., Trigoni, V. E. [et al]. Research and design of an aerodrome: Textbook for universities. Ed. by G. I. Glushkov. 2nd ed. Moscow, Transport publ., 1992, 463 p.



Table 3

Time interval values for assessing runway occupancy

Time interval	Value, s
Time of taxiing to the line-up position t_{taxi}	30...60
Time of stay of the aircraft at the line-up position to bring the engine thrust to take-off mode t_{th}	30...60
Aircraft takeoff run time t_{trun}	10...20
Time of acceleration and gaining the altitude t_{ag}	10...25
Aircraft gliding time from the decision altitude until touching down the runway t_{gl}	15...30
Aircraft landing run time t_{lrun}	15...25
Time of aircraft taxiing after landing beyond the side boundary of the runway (LOC critical area) T_{lrun}	30...60



Pic. 7. Curvature of the course lines and glide path of the ILS system of Gorno-Altai aerodrome for the existing aerodrome environs' area.

adopted in accordance with the condition of reducing speed and possible waiting before occupying PS, specified in the AIP.

Thus, the runway occupation time will be 80...165 s during takeoff and 60...115 s during landing. These time intervals can be reduced by reducing the taxiing to the line-up position and taxiing after landing. To solve this problem, it is necessary to expand the apron, which will make it possible not to reduce the speed when taxiing and to occupy parking stands PS2–PS6 and PS10 without the risk of blocking the path for the next aircraft. This solution requires a reduction in the size of LOC critical area, so it is advisable to

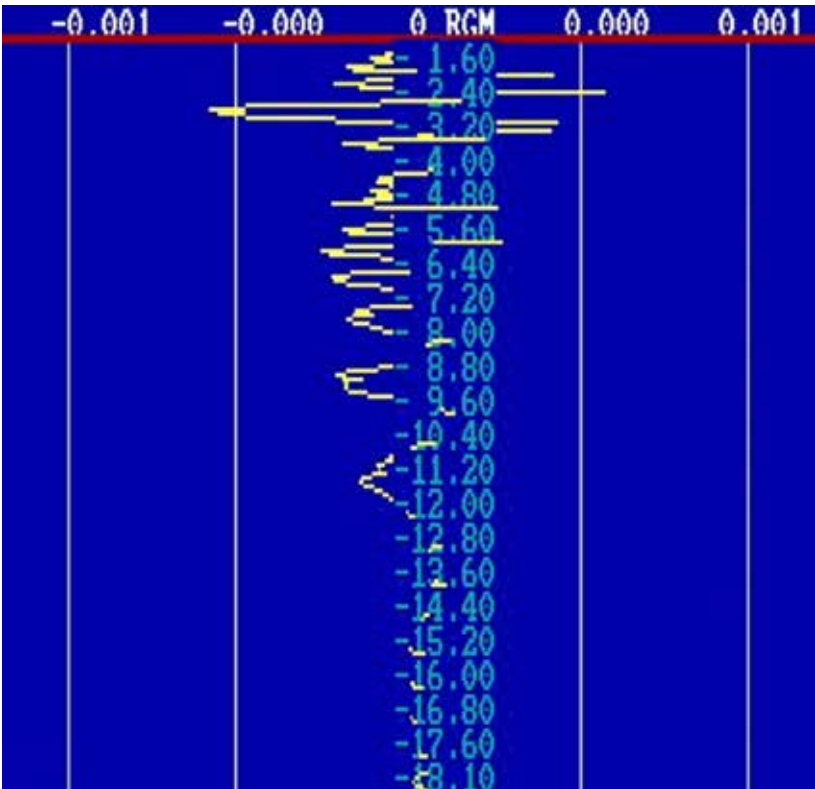
assess the feasibility of this solution and the possible impact of objects on the operation of the ILS.

We will use the developed algorithm, which includes 5 steps.

1. Let us evaluate the curvature of the course and glide path lines for the existing aerodrome environs' area using (5) and (6). Buildings and structures (Pic. 6) are objects of simple shape that can be approximated by the model of a reflecting object in the form of a wall; the elevated terrain is approximated by the model of a hemispherical diffuse reflecting object. We will present the results of the analysis in the form of



Pic. 8. Positioning of aircraft with dimensions corresponding to the Boeing-737 near the border of the LOC critical area.



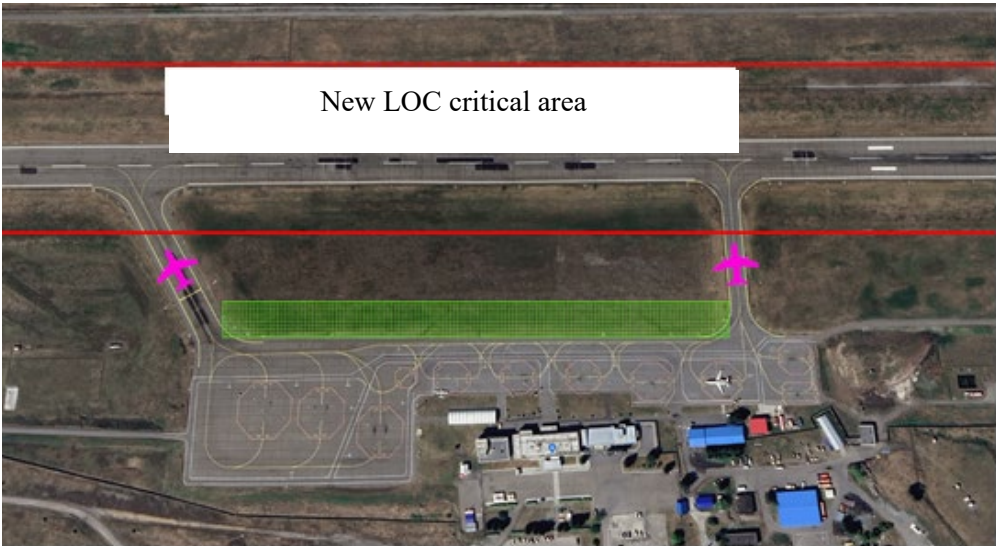
Pic. 9. Curvature of the course line of the ILS system of Gorno-Altai aerodrome when the Boeing-737 is located near the border of the LOC critical area.

graphs of curvature of the course and glide path lines, expressed in DDM units (Pic. 7).

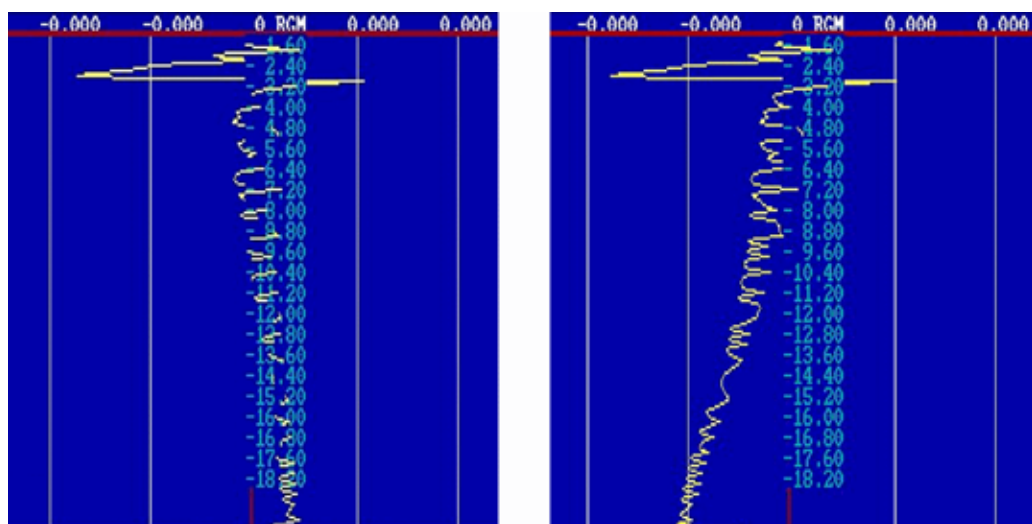
2. The results obtained allow us to conclude that Category I requirements have been met, which confirms the results of the flight check. Thus, the applied methodology provides an

adequate assessment for the conditions of Gorno-Altai aerodrome.

3. Let us evaluate the curvature of the course line when an aircraft with dimensions corresponding to the Boeing-737 is located near the border of the LOC critical area (Pic. 8). The



Pic. 10. Option for the expanded apron of Gorno-Altai aerodrome (a new LOC critical area and location of the objects under study are indicated).



Pic. 11. Curvature of the course line caused by aerodrome vehicles (car and tractor models).

results of the analysis are presented in Pic. 9. It can be seen that the curvatures do not go beyond the requirements of category I, thus, large reflecting objects do not cause significant distortions of the course line, which confirms the adequacy of the specified critical areas, the dimensions of which correspond to the requirements of FAP-297.

4. Let us evaluate the impact of objects for the reduced LOC critical area. The reduction in the boundaries of the LOC critical area is caused by the need to expand the apron. Pic. 10 shows a possible version of a new apron (the width has been increased by 30 m), as well as the boundaries of a new LOC critical area (the distance from the runway axis has been reduced to 80 m) and the location of objects. This will optimise taxiing procedures and also make it possible to modernise parking areas to receive heavy aircraft.

Let us evaluate the curvature of the course line for the following objects:

- aerodrome vehicles (car and tractor models);
- for light aircraft (L410);
- for medium aircraft (CRJ200);
- for heavy aircraft (Boeing-737).

At Gorno-Altai aerodrome there are no facilities that require the use of methods for assessing ESA of reflecting objects of various shapes, given in Table 1. There are no structures that require the use of a model of a complex object either (Pic. 4). Therefore, in this example, a simplified calculation is used: the technique is approximated by a model of a vertical wall, and

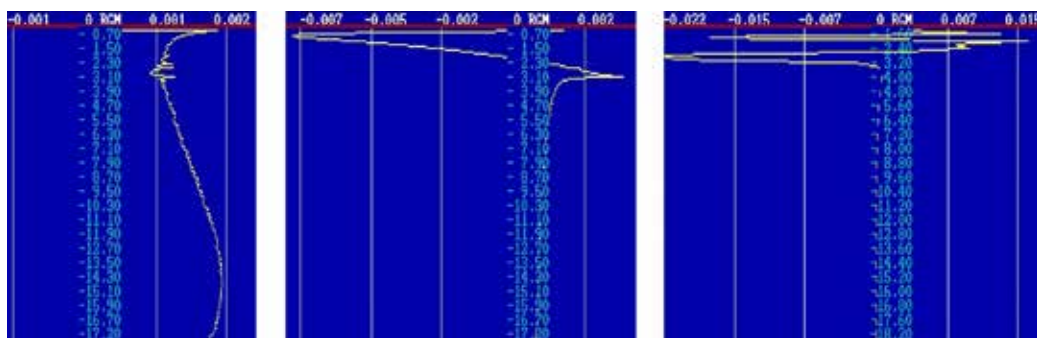
the aircraft is approximated by a model of a horizontal cylinder (fuselage) and a vertical wall (tail). For a more accurate calculation, it is recommended to take into account the complex shape of objects, as well as their structure. The simulation results are presented in Pics. 11 and 12.

5. The simulation results (Pics. 11 and 12) show that when placing objects (aerodrome vehicles and aircraft of various classes) in the positions shown in Pic. 10, the curvature of the course line does not exceed the standard values for category I. It can be concluded that it is possible to reduce the size of the LOC critical area in accordance with ICAO recommendations.

DISCUSSION

During further studies, it is planned to refine the presented methodology by including factors not previously considered in the analysis, which will increase the accuracy and reliability of the results. In this case, one should take into account the mathematical complexity of the modernised methodology, as well as the possibility of its implementation in the form of a software package.

Let's look at some analogues. Currently, methods have been developed and implemented for assessing and considering the curvature of the course and glide path lines for the ILS system. Thus, Airbus, together with the French National School of Civil Aviation (Ecole Nationale de l'Aviation Civile, ENAC) and the European Aeronautic Defense and Space Company



Pic. 12. Course line curvatures caused by light, medium and heavy aircraft.

(EADS), has developed software products: ATOLL and LAGON, which allow modelling the impact of terrain and local objects on operation of the ILS system using the physical optics method [1].

The work [7] has applied the ATOLL program to assess the influence of the designed building and construction cranes (with different boom rotation angles) on the LOC operation at Riga aerodrome. The modelling method has helped to prove that the new building will allow maintaining the existing landing category, however, during construction it is necessary to select placement points for construction cranes and monitor the angle of rotation of their booms when the aircraft is landing, as this can lead to unacceptable curvatures of the course line.

Study is also underway on the use of the method of moments and the multilevel multipole method. At the same time, in [1] it is noted that these methods have a number of constraints, in particular, they are not able to consider the influence of the underlying surface in the form of a ledge. In general, considering the underlying environment (slope in the longitudinal and transverse directions, uneven microrelief, the presence of snow or vegetation and its heterogeneity) is a separate area of research [13–15], and in the future it will have to be used within promising methods for assessing the curvature of the ILS course line and glide path.

CONCLUSION

Following the improvements in the features of ILS systems, the sizes of ILS critical areas (regulated by FAP-297) can be reduced. ICAO documents present the recommended sizes of critical areas, and it is noted that it is preferable to model the influence of objects on LOC and GP operation.

The article has presented a method for assessing the curvature of course and glide path lines and developed an algorithm for its application. Using the example of Gorno-Altaiisk aerodrome, an assessment has been made of the influence of objects located within the existing LOC critical area. It has been proven that the LOC critical area can be reduced, which will make it possible to expand the apron by 35 m and eliminate the current problem with limiting taxiing speed and blocking the movement of aircraft with a wingspan of more than 25...29 m when occupying aircraft parking stands PS2–PS6 and PS10.

When expanding the apron, it will be possible to obtain a probability of denial of service in the range of 0,001...0,003 (at TOL intensity of 10 aircraft/hour) and 0,05...0,105 (at TOL intensity of 15 aircraft/hour), which is 3...11 times less than the existing probability.

The expansion of the apron will make it possible not to reduce the taxiing speed and eliminate waiting time for aircraft when parking stands PS2–PS6 and PS10 are occupied. Thus, the time of taxiing before takeoff and after landing will be reduced to approximately 20...40 and 15...30 s. This will lead to a reduction in runway occupancy time to 70...145 s during takeoff and 45...85 s during landing, which is 12.5...26 % better than existing indicators. Improved performance (probability of service failure and runway occupancy time) will increase the aerodrome's capacity.

Since FAP-297 defines fixed sizes of the LOC and GP critical areas, it is recommended to amend existing regulations to take into account ICAO recommendations and ensure the possibility of reducing the ILS critical areas while maintaining a required level of flight safety.



It is necessary to identify cases requiring mandatory flight inspection of new critical areas and develop a program of special flight inspections. It is also necessary to identify cases that allow establishing the boundaries of critical areas based on simulation results and develop a single methodology and algorithm for carrying out calculations.

In further research, it is planned to modernise the methodology for assessing the curvature of the course and glide path lines to take into account additional factors, including the characteristics of the underlying surface that affect the spatial characteristics of the LOC and GP radiation.

REFERENCES

1. Voytovich, N. I., Ershov, A. V., Yungaitis, E. M. Diffraction of electromagnetic waves on a half-plane in relation to the aircraft landing system on aerodromes with a high level of snow cover and difficult terrain in the approach zone. *Journal of the Ural Federal district. Information security*, 2022, Iss. 1 (43), pp. 11–21. DOI: 10.14529/secur220102.
2. Tong, Kuang; Song, Yang; Kong, Xiangfen; Zhang, Kaiwen; Chen, Zijian. An integrated method for accurate identification and dynamic monitoring of buildings in aerodrome obstacle free space. ICAS 2020, pp. 1–14. [Electronic resource]: https://icas.org/ICAS_ARCHIVE/ICAS2020/data/papers/ICAS2020_1061_paper.pdf. Last accessed 17.06.2023.
3. Mitsevlch, L., Zhukovskaya, N. Geospatial modeling, analysis and mapping for aerodrome land. E3S Web of Conferences, 2021, Vol. 310. EDP Sciences, pp. 1–10. DOI:10.1051/e3sconf/202131004003.
4. Rubtsov, E. A. Automation of assessment of the impact of construction projects on operation of radio equipment for flight support [Avtomatizatsiya otsenki vliyaniya obektov stroitelstva na rabotu sredstv radiotekhnicheskogo obespecheniya poletov]. *I-methods*, 2022, Vol. 14, Iss. 3. [Electronic resource]: <http://intech-spb.com/wp-content/uploads/archive/2022/3/4-rubcov.pdf>. Last accessed 17.06.2023.
5. Iungaitis, E. M., Ershov, A. V., Zhdanov, B. V., Voytovich, N. I. Curvature of a radio engineering glide path as a holographic portrait of the terrain. *Microwave technology and telecommunication technologies (KryMiKo'2019)*, Sevastopol, 2019, pp. 43–48. EDN: SRRJO.
6. Iungaitis, E. M., Ershov, A. V., Zhdanov B. V., Voytovich, N. I., Zotov, A. ILS Glide Slope Antenna Array for Airfields with a High Level of Snow Cover. 13th European Conference on Antennas and Propagation, EuCAP 2019. Krakow, 2019, 8740267. [Electronic resource]: <https://ieeexplore.ieee.org/document/8740267>. Last accessed 17.06.2023.
7. Vorontsov, K., Lacane, M. A. Case Study for Riga International Airport Modernization: ILS Localizer Signal Accuracy Depending on Ground Obstacles Located Nearby. International Conference on Reliability and Statistics in Transportation and Communication. Springer, Cham, 2020, pp. 235–245. DOI: 10.1007/978-3-030-68476-1.
8. Zotov, A. V., Zhdanov, B. V., Voytovich N. I. Theory and experiment of ILS localizer course line electronic adjustment. 2019 International Conference on Industrial Engineering, Applications and Manufacturing, ICIEAM 2019. Sochi, 2019, 8743091. DOI: 10.1109/ICIEAM.2019.8743091.
9. Vozhdaev, V. V., Teperin, L. L. Characteristics of radar signature of aircraft [Kharakteristiki radiolokatsionnoi zametnosti letatelnykh apparatov]. Moscow, FIZMATLIT, 2018, 376 p. ISBN 978-5-9221-1782-1.
10. Ryapolov, I. E., Vasilets, V. A., Sukharevsky, O. I., Tkachuk, K. I. High-frequency method for calculating secondary radiation of a fuselage model of an unmanned aerial vehicle [Vysokochastotnyy metod rascheta vtorichnogo izlucheniya modeli fyuzelyazha bespilotnogo letatel'nogo apparata]. *Sistemi ozbroeniya i viiskova tekhnika*, 2014, Iss.1 (37), pp. 222–225. [Electronic resource]: https://www.researchgate.net/publication/370806235_VYSOKOCASTOTNYJ_METOD_RASCETA_VTORICNOGO_IZLUCENIYA_MODELI_FUZELAZA_BESPILOTNOGO_LETATELNOGO_APPARATA. Last accessed 17.06.2023.
11. Sukharevsky, O. I., Vasilets, V. A., Kukobko, S. V. [et al]. Scattering of electromagnetic waves by air and ground radar objects: Monograph [Rasseyaniye elektromagnitnykh voln vozduzhnymi i nazemnymi radiolokatsionnymi obektami: Monografiya]. Ed. by Sukharevsky, O. I. Kharkov, KhUPS, 2009, 468 p. ISBN 978-9-6646-8040-7.
12. Nechitaylo, S. V., Orlenko, V. M., Sukharevsky, O. I., Vasilets, V. A. Electromagnetic Wave Scattering by Aerial and Ground Radar Objects. SRC Press Taylor & Francis Group, Boca Raton, USA. 2014, 334 p. ISBN 9781315214511.
13. Zotov, A. V. Study of the influence of terrain on the output characteristics of the localizer of the instrumented landing system for aircraft. Abstract of Ph.D. (Eng) [Issledovanie vliyaniya relefa mestnosti na vykhodnye kharakteristiki kursovogo radiomayaka sistemy instrumentalnoi posadki samoletov. Avtoref. diss. kand. tekhn. nauk]. Yekaterinburg, 2017, 22 p. [Electronic resource]: <https://dspace.susu.ru/xmlui/bitstream/handle/0001.74/13585/000555376.pdf?sequence=1&isAllowed=y>. Last accessed 17.06.2023.
14. Iungaitis, E. M., Voytovich, N. I., Golovnin, A. A., Zhdanov, B. V. The influence of terrain in the form of a ledge on the behaviour of the trajectory for aircraft landing. *Microwave technology and telecommunication technologies (CriMiKo'2017): Proceedings of the 27th International Crimean Conference. In 9 volumes, Sevastopol, September 10–16, 2017. Volume 2*. Sevastopol, Sevastopol State University, 2017, pp. 379–386. EDN: YNKSNY.
15. Iungaitis, E. M., Zhdanov, B. V., Ershov, A. V., Voytovich, N. I. Behaviour of the information parameter of the glide slope of the aircraft landing system. *Microwave technology and telecommunication technologies*, 2020, Iss. 1–2, pp. 74–75. EDN: IDPLUN.

Information about the authors:

Rubtsov, Evgeny A., Ph.D. (Eng), Deputy Director of the Academy of Civil Aviation of Russian University of Transport, Moscow, Russia, rubtsov.rut.miit@yandex.ru.

Kudryakov, Sergey A., D.Sc. (Eng), Senior Researcher, Director of Scientific and Educational Centre for Air Transport of Russian University of Transport, Moscow, Russia, psi_center@mail.ru.

Dalinger, Iakov M., Ph.D. (Eng), Vice-Rector of Russian University of Transport, Moscow, Russia, iakovdalinger@gmail.com.

Article received 29.05.2023, approved 01.10.2023, accepted 09.10.2023.